Texture Preserving Variational Denoising Using an Adaptive Fidelity Term

Guy Gilboa, Yehoshua Y. Zeevi

Nir Sochen

Department of Electrical Engineering,
Technion - Israel Institute of Technology
Technion city, Haifa 32000, Israel
e-mail: {gilboa@tx,zeevi@ee}.technion.ac.il

Department of Applied Mathematics,
University of Tel-Aviv
Ramat-Aviv, Tel-Aviv 69978, Israel
e-mail: sochen@math.tau.ac.il

Abstract

Denoising algorithms based on gradient dependent energy functionals, such as Perona-Malik and total variation denoising, modify images towards piecewise constant functions. Although edge sharpness and location is well preserved, important information, encoded in image features like textures or certain details, is often compromised in the process of denoising. We propose a mechanism that better preserves fine scale features in such denoising processes. This is accomplished by adding a spatially varying fidelity term that locally controls the extent of denoising over image regions according to their content. Local variance measures of the oscillatory part of the signal are used to compute the adaptive fidelity term. Our results show improvement in the signal-to-noise ratio over scalar fidelity term processes, and they are more appealing visually. This type of processing is relatively simple, can be used for a variety of tasks in PDE-based image processing and computer vision, and is stable and meaningful from a mathematical viewpoint.

1 Introduction

PDE-based methods have been widely used over the past decade for image denoising with edge preservation. These methods are either based on the axiomatic approach of nonlinear scale-space (nonlinear diffusions), or on the variational approach of energy functional minimization. Details regarding the interaction and close relations between these approaches can be found, for example, in [14, 16].

A classical variational denoising algorithm is the total variation (TV) minimizing process of Rudin-Osher-Fatemi [9]. This algorithm seeks an equilibrium state (minimal energy) of an energy functional comprised of the TV norm of the image I and the fidelity of this image to the noisy input image I_0:

$$E_{TV} = \int_\Omega (|\nabla I| + \frac{1}{2}\lambda(I - I_0)^2)dxdy. \quad (1)$$

This is further generalized by the Φ-formulation [2, 4] with the functional

$$E_\Phi = \int_\Omega \left(\Phi(|\nabla I|) + \frac{1}{2}\lambda(I - I_0)^2 \right) dxdy. \quad (2)$$

The Euler-Lagrange (E-L) equation is

$$F \equiv \text{div}\left(\Phi' \frac{\nabla I}{|\nabla I|} \right) + \lambda(I_0 - I) = 0 \quad (3)$$

where $\lambda \in \mathbb{R}$ is a *scalar* controlling the fidelity of the solution to the input image (inversely proportional to the measure of denoising). Neumann boundary conditions are assumed. The solution is usually found by a steepest descent method:

$$I_t = F, \quad I|_{t=0} = I_0. \quad (4)$$

When the noise is approximated by an additive white Gaussian process of standard deviation σ, the problem can be formulated as finding

$$\min_I \int_\Omega \Phi(|\nabla I|)dxdy$$
$$\text{subject to } \frac{1}{|\Omega|} \int_\Omega (I - I_0)^2 dxdy = \sigma^2. \quad (5)$$

In this formulation, λ can be considered as a Lagrange multiplier, computed by:

$$\lambda = \frac{1}{\sigma^2|\Omega|} \int_\Omega \text{div}\left(\Phi' \frac{\nabla I}{|\nabla I|} \right) (I - I_0)dxdy. \quad (6)$$

The actual function with which we work in this paper is $\Phi(s) = \sqrt{1 + \beta^2 s^2}$. The process that results from this function is more stable than the TV. We choose it as a representative of variational denoising processes.

Although the performance of this, and other PDE-based methods, have shown impressive results, the limitations of such processes have recently become of great concern [3, 6, 12]. The implicit assumption that underlies the formulation of these flows/equations is the approximation of images by piecewise constant functions (in the BV space). In some sense they produce an approximation of the input image as the so-called "cartoon model" and, thus, naturally dispose of the oscillatory noise while preserving edges (in some cases even enhancing them, e.g. [8]).

A good cartoon model captures much of the image important information. Yet, it has several obvious drawbacks: textures are excluded, significant small details may be left out, and even large-scale fine features, that are not characterized by dominant edges, are often disregarded.

The purpose of this paper is to show that a relatively simple modification of the above equation yields a denoising algorithm that better preserves the structural (texture) information of the image.

2 The Cartoon Pyramid Model

The cartoon model has been defined and investigated in the early 80's [5, 1], was further elaborated by Mumford [7] and is widely used as the basic underlying model for many image denoising methods. In the continuous case, the cartoon has a curve Γ of discontinuities, but everywhere else it is assumed to have a small or a null gradient $|\nabla I|$.

The TV and other nonlinear diffusion processes are especially good in extracting the cartoon part of the image. We use them, therefore, as a simple pyramid (scale-space) of rough image sketches at different scales. Let us define a cartoon of scale s, using the Φ process, as follows:

$$C_s \doteq I_\Phi|_{\lambda = \frac{1}{s}} \qquad (7)$$

where I_Φ is the steady state of (**??**). Let us define the residue as the difference between two scales' cartoons:

$$R_{n,m} \doteq C_n - C_m \quad (n < m). \qquad (8)$$

We shall refer to the Non-Cartoon part of scale s as the residue from level zero:

$$NC_s \doteq R_{0,s} = C_0 - C_s. \qquad (9)$$

This cartoon and residue data structure is analogous of the pyramid of wavelet approximations. By using the definitions of (7) and (8) and integrating the E-L equation (3) we deduce the following basic properties:

1. $C_0 = I_0$
   (The cartoon of scale 0 is the input image).
2. $C_\infty = \int_\Omega I_0(x, y) dx dy$
   (The cartoon of scale ∞ is the mean of the input image).
3. $\int_\Omega R_{n,m} dx dy = 0$
   (The mean of any residue is zero).
4. $C_s = \int_s^\infty R_{n,n+dn} dn + C_\infty$
   $= \Sigma_{n=s}^\infty R_{n,n+1} + C_\infty$
   (A cartoon image can be built from residues
   of larger scales).

The Φ diffusion process dissipates energy. We note that the term $\int_\Omega (I_0 - I)^2 dx dy$ is, actually, the power of the residue. This implies that I_Φ can be viewed as the most non-oscillatory sketch of I_0 when the permitted reduced power of the original signal is bounded by some measure proportional to $\frac{1}{\lambda}$.
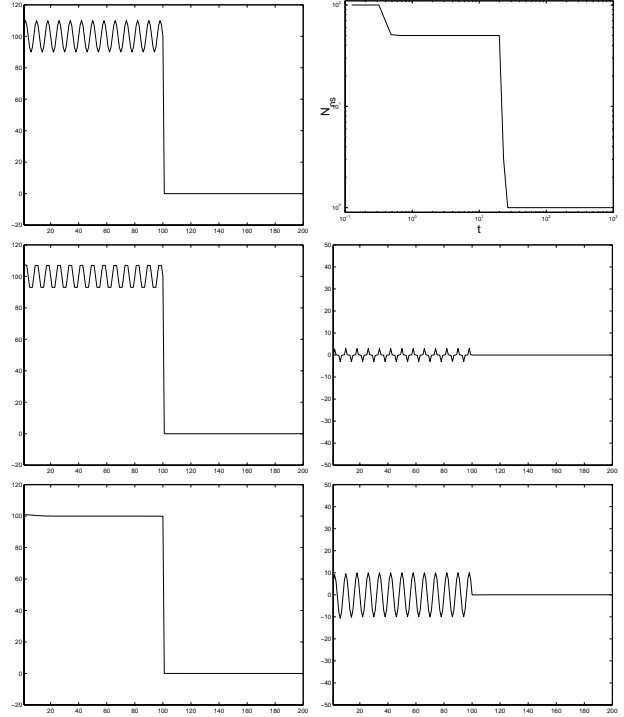
Figure 1: Top row: Original signal I_{orig} (left), non-smoothness $|N_{ns}|$ as a function of evolution time (right), middle row: Signal (left) and residue (right) of first stable scale, bottom row: Signal (left) and residue (right) of second stable scale.
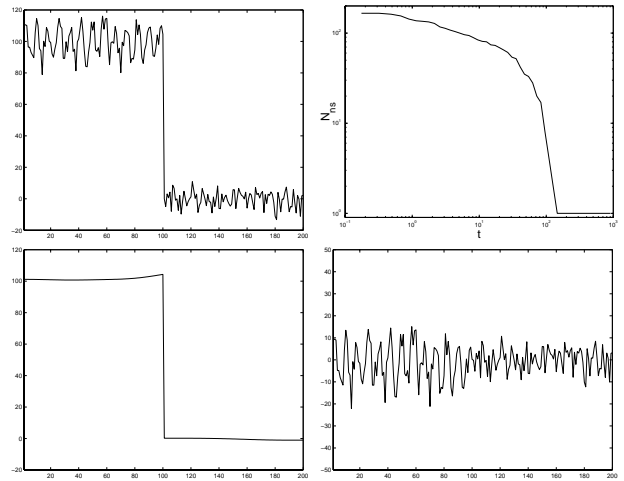
Figure 2: Top: Noisy signal I_0 (left), non-smoothness $|N_{ns}|$ as a function of evolution time (right), bottom: signal (left) and residue (right) of stable scale.

In order to model a natural image in a simple way, yet capture its significant characteristics, we model the image as a cartoon of a single scale with its matching residue. We refer to the scale so chosen, to represent the cartoon part of the im-

Figure 3: An example of processing results obtained with a natural image. From top: Original 'Barbara image' (left); Noisy version of the original image, I_0, with SNR=8.7dB, $\sigma = 20$ (right); Result of processing with scalar λ (SNR=12.6dB, left); Result of processing with adaptive λ (SNR=14.2dB, right); Residue I_R (left); $S(x, y)$ calculated according to residue (middle) $\lambda(x, y)$ at convergence of process (right).
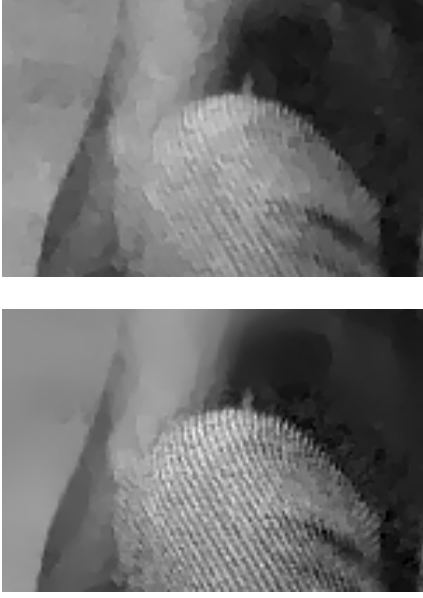
Figure 4: Enlargement of Barbara's right knee (full images are in Fig. 3). Top - result of scalar process, bottom - result of adaptive process.

age, as the representative cartoon scale s_r. There can be several approaches to finding a representative scale, and, in general, an image can have several such scales. We propose to find the representative scale by examining the stability of the gradients along scales. As a cartoon consists primarily of a piecewise smooth image, partitioned by edges, a stable scale range $[s_1, s_2]$ is one in which the total edge length (number and size of objects) changes very slowly. As the definition of an edge is not always clear, we resort to finding the smooth regions defined as having a gradient of less then 1% of the dynamic range of the input image. The total area (length in 1D) of smooth regions is $|N_s| = \int_\Omega \chi(N_s) dx dy$ where $\chi(A)$ is the indicator function of the set A, and we define the set of smooth points as $N_s \doteq \{(x,y) : |\nabla I(x,y)| < T_s\}$. Here $T_s = (\max_\Omega(I_0) - \min_\Omega(I_0))/100$. The set of non-smooth points is $N_{ns} = \Omega - N_s$. The smoothness area $|N_s|$ is generally increasing in scale ($|N_{ns}|$ decreasing), though monotonicity of the area, and embedding of the sets, is not guaranteed. For monotone Lyapunov functionals that can indicate stability of scales see [15]. We choose the scale s_r as one of the meta-stable states of $|N_s|$ (Figs. 1,2).

Our model consists of three components: $I_0 = I_C + I_{NC} + I_n$, where $I_{orig} = I_C + I_{NC}$ is the original image, I_C is the Cartoon approximation, I_{NC} is the remainder Non-Cartoon part, and I_n is an additive noise. Note that we left the definition of "non-cartoon" part vague. It, typically, consists of textures, small-scale details, thin lines etc. The only assumption we make is that it has zero mean. Under this decomposition, the residue of the noisy image is:

$$I_R \equiv I_0 - I = \tilde{I}_{NC} + \tilde{I}_n . \qquad (10)$$

Note that we distinguish between the "true" non-oscillatory part and its approximation by the Φ diffusion process by the tilde upperscript.

3 The Adaptive Φ Problem

To obtain an adaptive scheme, we generalize the Φ denoising problem by imposing a spatially varying power constraint. Let us define first a measure to which we refer as the *local power*:

$$P_z(x,y) \equiv \frac{1}{|\Omega|} \int_\Omega (I_z(\tilde{x}, \tilde{y}) - \eta[I_z])^2 w_{x,y}(\tilde{x}, \tilde{y}) d\tilde{x} d\tilde{y}, \qquad (11)$$

where $w_{x,y}(\tilde{x}, \tilde{y}) = w(|\tilde{x} - x|, |\tilde{y} - y|)$ is a normalized ($\int_\Omega w_{x,y}(\tilde{x}, \tilde{y}) d\tilde{x} d\tilde{y} = 1$) and radially symmetric smoothing window, $\eta[\cdot]$ is the expected value. From the definition of the local power it follows that $\int_\Omega P_z(x,y) dx dy = \mathcal{P}_z$, where

$$\mathcal{P}_z \equiv \text{var}(I_z). \qquad (12)$$

We reformulate the scalar Φ problem, stated in Eq. (5), in the context of the adaptive Φ problem as follows:

$$\begin{aligned} &\min_I \int_\Omega \Phi(|\nabla I|) dx dy \\ &\text{subject to } P_{\hat{R}}(x,y) = S(x,y), \end{aligned} \qquad (13)$$

where $I_{\hat{R}} = (I - I_0 - C)$, C is a constant and $S(x,y) \geq 0$ is assumed to be given a-priori.

We solve the optimization problem using Lagrange multipliers:

$$E = \int_\Omega \left(\Phi(|\nabla I|) + \frac{1}{2}\lambda(x,y)P_{\hat{R}}(x,y) \right) dx dy. \qquad (14)$$

The Euler-Lagrange (EL) equation for the variation with respect to I is

$$\bar{\lambda}(x,y)(I - I_0 - C) - \text{div}\left(\Phi' \frac{\nabla I}{|\nabla I|} \right) = 0, \qquad (15)$$

where for any quantity $X(x,y)$ we define the locally averaged quantity $\bar{X}(x,y) = \int_\Omega X(\tilde{x}, \tilde{y}) w_{x,y}(\tilde{x}, \tilde{y}) d\tilde{x} d\tilde{y}$. We solve this equation for I by a gradient descent:

$$I_t = \bar{\lambda}(x,y)(I_0 - I + C) + \text{div}\left(\Phi' \frac{\nabla I}{|\nabla I|} \right). \qquad (16)$$

In order to compute the value of λ we multiply the EL equation (15) by $(I - I_0 - C)$ and integrate over. After a change in the order of integrals in the λ term we get

$$\int_\Omega (\lambda(x,y)S(x,y) - Q(x,y)) dx dy = 0, \qquad (17)$$

where

$$Q(x,y) = (I - I_0 - C)\text{div}\left(\Phi' \frac{\nabla I}{|\nabla I|} \right).$$

A sufficient condition is

$$\lambda(x, y) = \frac{Q(x, y)}{S(x, y)}. \quad (18)$$

Finally, the constant C is obtained by solving $\partial_C E = 0$, yielding

$$C = \frac{\int_\Omega \lambda(x, y)(\bar{I}(x, y) - \bar{I}_0(x, y))dxdy}{\int_\Omega \lambda(x, y)dxdy}. \quad (19)$$

3.1 Automatic Texture Preserving Denoising

In the general case, we do not have any significant prior knowledge on the image that can facilitate the denoising process. We only assume that the noise is of constant power, and is not correlated to the signal (e.g. additive white Gaussian or uniform noise).

Our aim is to use the Φ denoising mechanism in a more accurate and precise manner. Images which can be well represented by large scale cartoon model are the best candidates for successful denoising. Images with much fine texture and details will not benefit that much from the operation; while reducing most of the noise, this type of processing will inevitably degrade important image features. The first problem is to distinguish between good and bad candidates for Φ denoising. The task becomes even more complex if this is done adaptively. Many natural images exhibit a mosaic of piecewise smooth and texture patches. This type of image structure calls for position (spatial)-varying filtering operation.

The performance of the scalar Φ denoising process is illustrated in Fig. 5, using a typical cartoon-type and textured images. The SNR's of these three processed images are summarized in Fig. 6, and plotted as a function of the reduced power (normalized power of the residue). Obviously, as these examples illustrate, cartoon-type images are denoised much better than textured images (both in terms of SNR and visually). Another important observation is that the maximal SNR of cartoon and non-cartoon images is reached at different levels of denoising. Whereas cartoon-type images are stable and reach their peak SNR at high denoising levels ($\mathcal{P}_R \approx \sigma^2$), non-cartoon images degrade faster and require less denoising ($\mathcal{P}_R < \sigma^2$).

We present here a relatively simple method that can approximate the desired level of denoising in a region. In our above formulation (Eq. 13), the problem reduces to finding $S(x, y)$.

We use the cartoon pyramid model for this purpose. Our first aim is to differentiate between the cartoon part of the image I_C and the noise and texture parts $I_{NC} + I_n$. We choose the first meta-stable scale where $\mathcal{P}_R \geq \sigma^2$ (this condition is actually implicit as there is no stable scale with residue power below the noise level). We assign

$$S(x, y) = \frac{\sigma^4}{P_R(x, y)}, \quad (20)$$

where $P_R(x, y)$ is the local power of the residue I_R.
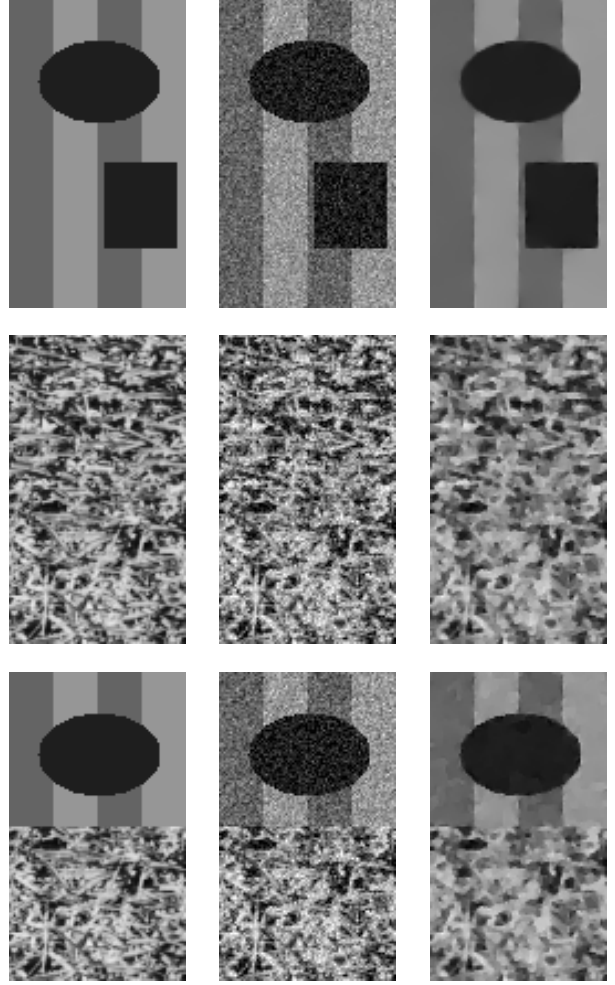
Figure 5: Scalar Φ denoising of textured and texture-free images. Top row: Piecewise constant image, middle row: Textured image of grass, bottom row: Patches of the two types of images combined in one. Left column depicts the original images, middle column - noisy images, right column - result of scalar Φ processing (Eq. 3) at convergence ($\mathcal{P}_R = \sigma^2$).

In the case where $I_R \approx I_n$ (basic cartoon model without textures or fine scale details) this scheme degenerates to the scalar Φ process. The local power of the residue is almost constant ($P_R(x, y) \approx \sigma^2$) and hence $S(x, y) \approx \sigma^2$. We get a high quality denoising process where $I \approx I_C = I_{orig}$. In the case of most natural images, however, textures will also be filtered and included in the residue part. As the noise is uncorrelated with the signal, we can approximate the total power of the residue as $P_{NC}(x, y) + P_n(x, y)$, the sum of local powers of the non-cartoon part and the noise, respectively. Thus, textured regions are characterized by high local power of the residue. In order to preserve the detailed structure of such regions, the level of filtering there should be minimized over these regions.
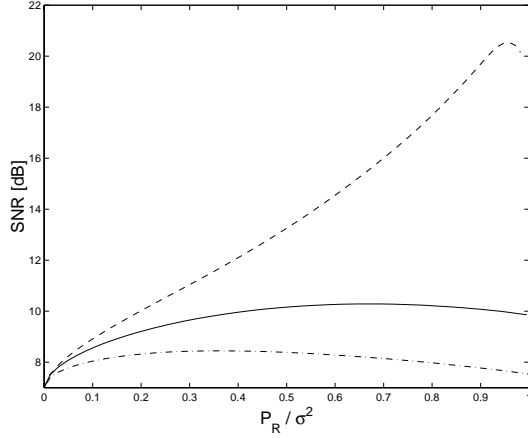
Figure 6: SNR of scalar Φ denoising of images shown in Fig. 5. SNR is plotted as a function of the reduced power, normalized by the noise power: $\mathcal{P}_R/\sigma^2$. Dashed line piecewise constant image, dash-dot line texture image, solid line combined image.

Let us recall the classical Wiener filter (optimal linear filter in the mean squared-error sense). Its formulation in the frequency domain is

$$G(\omega) = \frac{Ps(\omega)}{Ps(\omega) + Pn(\omega)}, \qquad (21)$$

where $Ps(\omega)$ and $Pn(\omega)$ are the power spectrum of the signal and noise, respectively. The basic concept amounts to reduction in the extent of filtering ($G \to 1$) at frequencies where the signal power exceeds that of the noise.

In our case we have a similar principle, whereby reduction in the extent of filtering (i.e. $S \to 0$) is called for in regions where signal power exceeds that power of the noise. The signal is in this case that portion of the image accounting for the texture and fine details that may be filtered out by the Φ process. Formally, substituting the relation $P_R(x, y) \approx P_{NC}(x, y) + P_n = P_{NC}(x, y) + \sigma^2$ for $P_R(x, y)$ in Eq. (20), we get

$$S(x, y) \approx \sigma^2 \frac{1}{1 + P_{NC}(x, y)/\sigma^2}. \qquad (22)$$

3.2 Denoising with prior information

In cases where more information regarding the structure of the original signal is available, the performance of denoising process incorporating a spatially-varying fidelity constraint can be substantially ameliorated. The specifics are application-dependent and heuristic in nature. We therefore mention here only a few related ideas. To preserve specific features in the denoising process, such as long thin line or known types of textures, one can pre-process with the corresponding feature detector (Hough transform, texture detector). The value of $S(x, y)$ depends, then, locally on the feature detector response. Cases of spatially varying noise also

fit the model. For example, in low-quality JPEG images, the boundaries between 8x8 pixel-blocks are often more noisy and fidelity of the original data there should, therefore, be decreased (S increased).
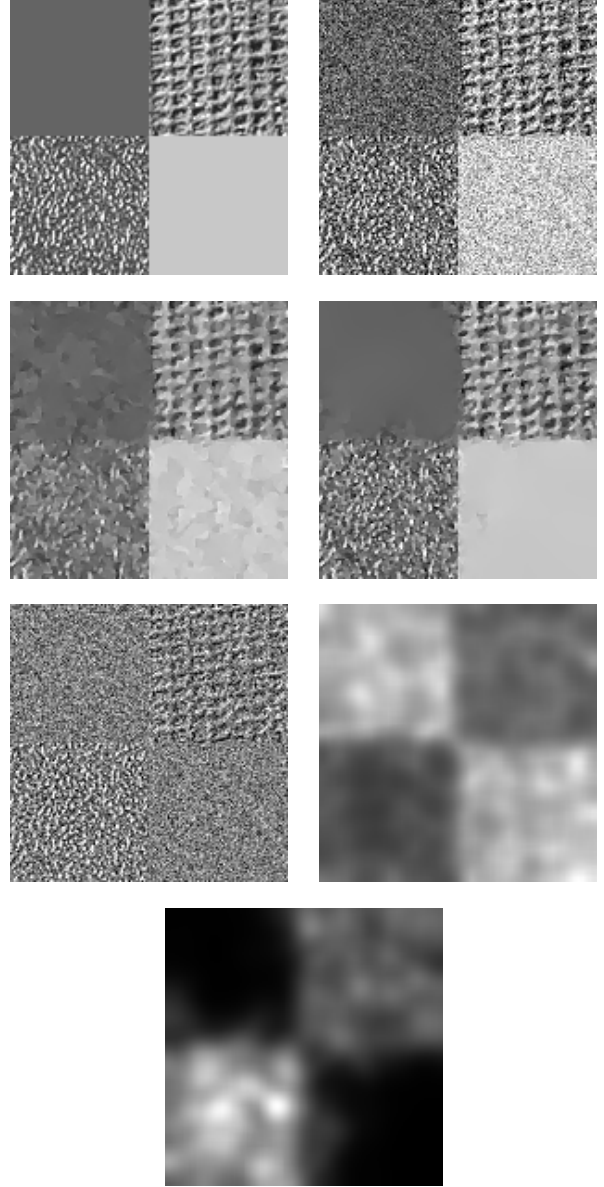
Figure 7: Processing of a noisy mosaic of textures (fabric and metal) and smooth areas. From top: Original mosaic made of patches of fabric and metal textures, juxtaposed with two constant patches (left); Noisy version, I_0, of the original with SNR=2.4dB, $\sigma = 40$ (right); Result of processing with scalar λ - SNR=6.4dB (left), result with adaptive λ - SNR=7.6dB (right); Residue I_R (left); $S(x, y)$ calculated according to the residue (right); $\lambda(x, y)$ at the convergence of the process (bottom image).

4 Examples

The effects of adaptive- versus scalar-fidelity denoising are illustrated using a synthetic mosaic comprised of two textured patches juxtaposed with two smooth patches (Fig. 7). The scalar fidelity term requires that a global power, equal to the noise power, be reduced. As the Φ process is smoothing both texture and noise, more power is reduced in the textured regions than in the originally smooth ones. This results in oversmoothing of textured regions, whereas smooth regions are not sufficiently denoised (Fig. 7, left side second row from top). The adaptive fidelity term process (second row right) applies different levels of denoising in different regions. This improves the result both visually (texture is better preserved, smooth regions are better denoised) and in terms of signal-to-noise ratio. At the third row of Fig. 7, we show how the required spatially varying noise power, $S(x, y)$ (right), depends on the value of the residue, I_R (left). The value of the adaptive fidelity term, $\lambda(x, y)$, obtained when the process converges is depicted graphically by the image at the bottom of the figure (lighter regions indicate higher value). Naturally, the value of $\lambda(x, y)$ is inversely related to the reduced power measure $S(x, y)$.

Processing a noisy version of the Barbara image (Fig. 3), it is demonstrated how the adaptive Φ method well performs on natural images. Our simple local power criterion seems to be sufficient to differentiate textured from smooth regions, even in relatively complex images. Accordingly, appropriate local requirements on the power to be reduced are applied. In Fig. 4, Barbara's right knee is enlarged to highlight similar phenomena to those obtained in the case of the synthetic example, where textures are preserved and the denoising of smooth regions is stronger. Fig. 8 shows the Teddy-bear from the Toys image where the textured bear parts are in front of a smooth background. Noise is reduced selectively in a natural manner.

In Table 1 we show the comparison between scalar and adaptive processes in terms of SNR. As can be observed, denoising is improved in a variaty of natural images.

4.1 Implementation details

We used explicit Euler schemes to implement the iterative processes. The averaging window $w(x, y)$ was selected to be a Gaussian of standard deviation $\sigma_w = 5$. The potential in all images was $\Phi(s) = \sqrt{1 + s^2}$ ($\beta = 1$). As we used gray level images with values in the range $[0, 255]$ the results are similar to TV denoising. We observed that the calculation of the constant C gives very little improvement. Therefore we used $C = 0$ to save time. The residue power was bounded by $\mathcal{P}_R \leq 1.5\sigma^2$. In the experiment on natural images (results shown in Table 1) we set a constant residue power $\mathcal{P}_R = 1.5\sigma^2$. Texture patches were taken from the VisTex archive [13]. All images were processed automatically with the same parameters (no tuning of parameters was performed for each image).

Figure 8: Part of the Toys image. Top left - original, top right - noisy image, bottom left - result of scalar denoising, bottom right - result of adaptive denoising.

Image	SNR_0	Scalar	Adaptive
Cameraman	15.8	19.2	**20.8**
Lena	13.5	17.5	**18.6**
Boats	15.6	19.6	**20.6**
Sailboat	10.4	15.1	**16.3**
Toys	10.0	16.8	**17.8**

Table 1: Denoising results of a few classical images. From left, SNR of the noisy image (SNR_0), SNR of scalar denoising ('Scalar'), SNR of adaptive denoising ('Adaptive'). All experiments were done on images degraded by additive white Gaussian noise ($\sigma = 10$).

5 Conclusion

The widely-used variational denoising algorithms with global power constraints well perform on simple cartoon-type images, where most of the information is represented by the simple skeleton approximation of the image. However, in order to preserve texture and small scale details, more subtle constraints are called for. We developed an adaptive variational scheme that controls the level of denoising by local power (variance) constraints.

In this study a simple mechanism based on the local power of the residue was introduced in order to determine the desired adaptive constraints. Solving the EL equations resulted in a spatially varying fidelity term that determines the value of the fidelity to the input image (or degree of denoising) in each region. A-priori knowledge on the details to be preserved can further enhance this method.

We have shown that this scheme can filter noise better than the scalar fidelity term process in terms of SNR over a variety of synthetic and natural images. Visually, the processed images look more natural and less 'cartoon-like'. Spatially varying power constraints can be used in almost any variational denoising process. Further improvement may be gained in distinguishing between texture and noise by using more elaborated schemes other than the power criterion, such as those obtained by transforming the residue to the Gabor/wavelet space.

Acknowledgments

References

[1] A. Blake, A. Zisserman, *Visual Reconstruction*, MIT Press 1987.

[2] L. Blanc-Féraud, P. Charbonnier, G. Aubert, M. Barlaud, "Nonlinear image processing: modelling and fast algorithm for regularization with edge detection", In Proc. IEEE ICIP-95, Vol. 1, pp. 474-477, 1995.

[3] T.F. Chan, J. Shen, "A good image model eases restoration - on the contribution of Rudin-Osher-Fatemi's BV image model", IMA preprints 1829, Feb. 2002.

[4] R. Deriche, O. Faugeras, "Les EDP en Traitement des Images et Vision par Ordinateur", Traitement du Signal, 13(6), 1996.

[5] S. Geman, D. Geman, "Stochastic relaxation, Gibbs distributions, and the Bayesian restoration of images", IEEE Trans. PAMI, vol. 6, pp. 721-741, 1984.

[6] Y. Meyer, *Oscillatory Patterns in Image Processing and Nonlinear Evolution Equations*, Vol. 22 University Lecture Series, AMS, 2001.

[7] D. Mumford, "The Bayesian Rationale for Energy Functionals", B M ter Haar Romeny Ed., *Geometry Driven Diffusion in Computer Vision*, Kluwer Academic Publishers, 1994.

[8] P. Perona, J. Malik, "Scale-space and edge detection using anisotropic diffusion", PAMI 12(7), pp. 629-639, 1990.

[9] L. Rudin, S. Osher, E. Fatemi, "Nonlinear Total Variation based noise removal algorithms", Physica D 60 259-268, '92.

[10] D.M. Strong, T.F. Chan, "Spatially and scale adaptive total variation based regularization and anisotropic diffusion in image processing", UCLA CAM Rep. 96-46, Nov. 1996.

[11] A. Tsai, A. Yezzi, A.S. Willsky, "Curve evolution implementation of the Mumford-Shah functional.." IEEE Trans. IP, 10(8), pp. 1169-1186, 2001.

[12] L.A. Vese, S.J. Osher, "Modeling textures with total variation minimization and oscillating patterns in image processing", UCLA CAM Report 02-19, May 2002.

[13] VisTex Vision Texture Archive of the MIT Media Lab, http://www-white.media.mit.edu/vismod/imagery/ VisionTexture/vistex.html

[14] J. Weickert, "A review of nonlinear diffusion filtering", B. ter Haar Romeny, L. Florack, J. Koenderink, M. Viergever (Eds.), Scale-Space Theory in Computer Vision, LNCS 1252, Springer, Berlin, pp. 3-28, 1997.

[15] J. Weickert, "Coherence-enhancing diffusion filtering", IJCV 31(2/3), 111-127, 1999.

[16] Y. You, W. Xu, A. Tannenbaum, M. Kaveh, "Behavioral analysis of anisotropic diffusion in image processing", IEEE Trans. Image Process, Vol. 5, No. 11, 1996.